PHILOSOPHICAL TRANSACTIONS OF THE ROYAL SOCIETY A MATHEMATICAL, PHYSICAL & ENGINEERING SCIENCES

Experiments with single atoms in a cabity: entanglement, Schrodinger's cats and decoherence

S. Haroche, M. Brune and J. M. Raimond

Phil. Trans. R. Soc. Lond. A 1997 **355**, 2367-2380
doi: 10.1098/rsta.1997.0133

Experiments with single atoms in a cavity: entanglement, Schrödinger's cats and decoherence

By S. Haroche, M. Brune and J. M. Raimond

Laboratoire Kastler Brossel, Département de Physique de l'Ecole Normale Supérieure, 24 rue Lhomond, F-75231 Paris, Cedex 05, France

We perform experiments with Rydberg atoms crossing one at a time a superconducting cavity containing a few microwave photons. The coupling between the atoms and the cavity field is either resonant or dispersive. In the resonant case, quantum Rabi oscillations induced by the vacuum or by a small coherent field are observed. These signals reveals in a striking way the quantization of the field. Quantum Rabi oscillations are also used to prepare Fock states of radiation, to transfer information or to produce entanglement between two successive atoms crossing the cavity. Dispersive atom–field coupling is used to prepare and probe coherent superpositions of field states with different phases (Schrödinger cat states). The progressive decoherence of these states is observed. These experiments constitute fundamental tests of quantum theory and shed light on the transition from quantum to classical in mesoscopic systems.

1. Introduction

It is now possible to realize with atoms and cavities experiments which would until recently have been considered of the purely 'Gedanken' type. These experiments correspond to the simplest atom–radiation coupling situation. They involve a single two-level atom interacting coherently with one mode of the field, either in its vacuum state, or containing only a few photons (Haroche 1992; Berman 1994). The observed signals illustrate the basic postulates of quantum mechanics and their analysis provide severe tests of our understanding of the least intuitive aspects of quantum theory, which involve in particular non-local entanglement and mesoscopic state superpositions. By allowing us to study how these state superpositions evolve into a mere statistical mixture as a function of the 'size' of the system under study, these experiments can also be viewed as a step towards the exploration of the transition from the quantum to the classical world (Zurek 1981, 1982, 1991, 1997). In this short presentation, we briefly describe the very versatile experimental set-up which has made these experiments possible and present a brief account of the most important results obtained so far.

2. The atom–cavity set-up

These experiments (Brune *et al.* 1996*a*,*b*; Hagley *et al.* 1997; Maître *et al.* 1997) require very long-lived systems, strongly coupled to each other, in a well-controlled

Phil. Trans. R. Soc. Lond. A (1997) **355**, 2367–2380
Printed in Great Britain

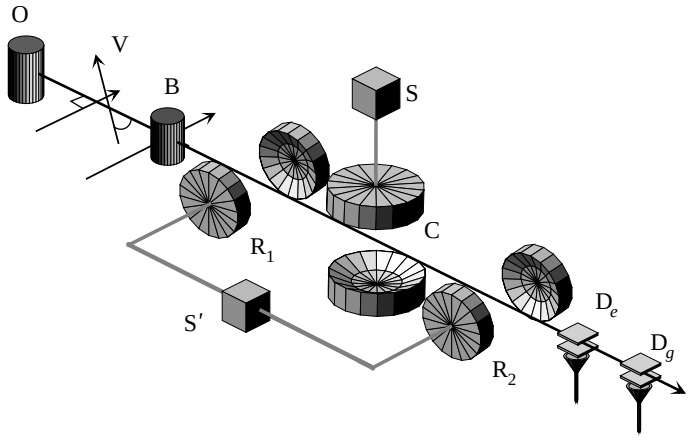

Figure 1. Scheme of the atom–cavity experimental set-up.

environment. We make use of superconducting microwave cavities resonant with a millimetric transition at 51 GHz coupling two adjacing circular Rydberg states of Rubidium (principal quantum numbers 51 and 50). The experimental set-up, whose core is cooled to 0.6 K by a ^{3}He–^{4}He cryostat, is sketched in figure 1. The cavity C is made of two spherical niobium mirrors facing each other in a Fabry–Perot configuration (distance between mirrors: 2.7 cm). The cavity sustains a TEM Gaussian mode with a 6 mm waist, and an effective volume of 0.7 cm^3. The field decay time is essentially determined by the smoothness of the mirror surface. Long damping times, of the order of several milliseconds, have already been obtained, but all the experiments described below have been performed with somewhat lower finesse cavities, whose damping time $T_{\rm cav}$ is comprised between 100 and 200 μs. The cavity field is excited either by the atoms themselves (resonant atom–field coupling), or externally, by a microwave source S. In this latter case, a coherent field is prepared in C. It is possible to tune the cavity in and out of resonance with the atomic transition by slightly changing the distance between the mirrors. Alternatively, one can tune by Stark effect the atomic transition frequency across the cavity resonance by varying the electric field applied across the mirrors (a non-zero average field must in any case be maintained between the mirrors in order to avoid the mixing of circular states with Rydberg levels of lower angular momentum while the atoms cross C (Hulet & Kleppner 1983; Nussenzveig *et al.* 1993)).

The circular Rydberg states $n = 51$ and 50 (called e and g, respectively, in the following) correspond to a very large circular orbit (diameter 0.125 μm) and have very long radiative damping times (30 ms). They behave as huge atomic antennae, strongly coupled to radiation. The atoms, initially effusing from an oven O, are optically pumped into one velocity class with the help of a laser beam exciting them at an angle with respect to the atomic beam propagation (Doppler tuning of the Rubidium resonance line in zone V). The atoms are then prepared in box B in one of the two states e or g by a succession of laser pulse excitations followed by adiabatic radiofrequency transitions feeding angular momentum into the atom (Nussenzveig *et al.* 1993). This preparation stage is pulsed, preparing bursts of circular atoms which emerge from B at well-defined times, with well-controlled velocities (comprised between 200 and 400 m s^{-1} with a ±0.4 m s^{-1} precision). The average number of atoms in each burst is kept much below one, so that the probability to prepare two atoms at a time remains small.

After preparation, the atoms enter a small auxiliary cavity R_1 in which a classical pulse of microwave is optionally applied, turning e or g into a linear superposition of these two states. The atoms then cross C during an interaction time in the few 10 μs range, shorter than the cavity field or atomic damping times. The coupling between the atoms and the field in C is defined by the vacuum Rabi frequency $\Omega/2\pi = 50$ kHz, which corresponds to the rate at which the cavity mode exchange a single photon with an atom located at cavity centre. When the atom moves across the cavity, Ω appears as a Gaussian function of the atom's position. Several Rabi oscillations can occur during the atom–cavity crossing time. After C, the atoms cross another auxiliary cavity R_2, where a pulse of classical resonant microwave may be applied, mixing again e or g. Finally, the atoms reach two field ionization detectors D_e and D_g counting atoms in level e or g, with a 40% quantum efficiency. The time resolution of the experiment allows us to know with a ±1 mm precision where each atom is in the apparatus at any time, making it possible to subject successive atoms to different interactions in R_1, C and R_2.

An experimental event consists in sending one atom, or two atoms separated by a well-defined time interval, across the system and detecting them downstream in D_e or D_g. The same sequence is repeated many times, with a repetition period longer than the cavity C damping time, so that the same initial field can be prepared in C at the beginning of each sequence. Results are obtained by extracting statistics from the repeated sequences (single atom probability or joint two atom probabilities of detecting the atoms in states e or g). A cavity with a very long damping time corresponds to a very small decoherence rate, but requires very low repetition rates and very long statistics acquisition times. In the experiments described below, in which the cavity damping time was moderately long (100–200 μs), the repetition period was 1.5 ms and samples used to extract joint two-atom probabilities corresponded typically to 15 000 useful events, recorded in about two hours.

3. Resonant atom–field coupling experiments

In a first series of experiments, the cavity mode was tuned in exact resonance with the $e \rightarrow g$ atomic transition, so that photons could be emitted or absorbed by each atom while it crossed C. This is a micromaser situation (Raithel *et al.* 1994) restricted to single atom–single photon interactions (Haroche *et al.* 1982). We have investigated in detail the phenomenon of quantum Rabi oscillation (Eberly *et al.* 1980). We have also used the atom–field resonant coupling to prepare and detect non-classical Fock states, to demonstrate the operation of a quantum field memory and to generate entanglement between successive atoms crossing the cavity.

(*a*) *Quantum Rabi oscillation: direct test of field quantization in a box*

The simplest experiment (Brune *et al.* 1996*a*) is performed by sending an atom in level e in the cavity and measuring the probability that the atom flips from e to g. The auxiliary microwave zones R_1 and R_2 are not used. The measurement is performed for various atom–cavity interaction times, which are obtained either by changing the velocity of the detected atoms, or by Stark tuning the atomic transition in resonance with the cavity mode during a fraction of the atom–cavity crossing time (in this experiment, the atom's velocity was not actively selected by optical pumping, as described above, but only passively determined by a time of flight measurement).

Figure 2*a* shows the Rabi oscillation signal versus time obtained when the cavity

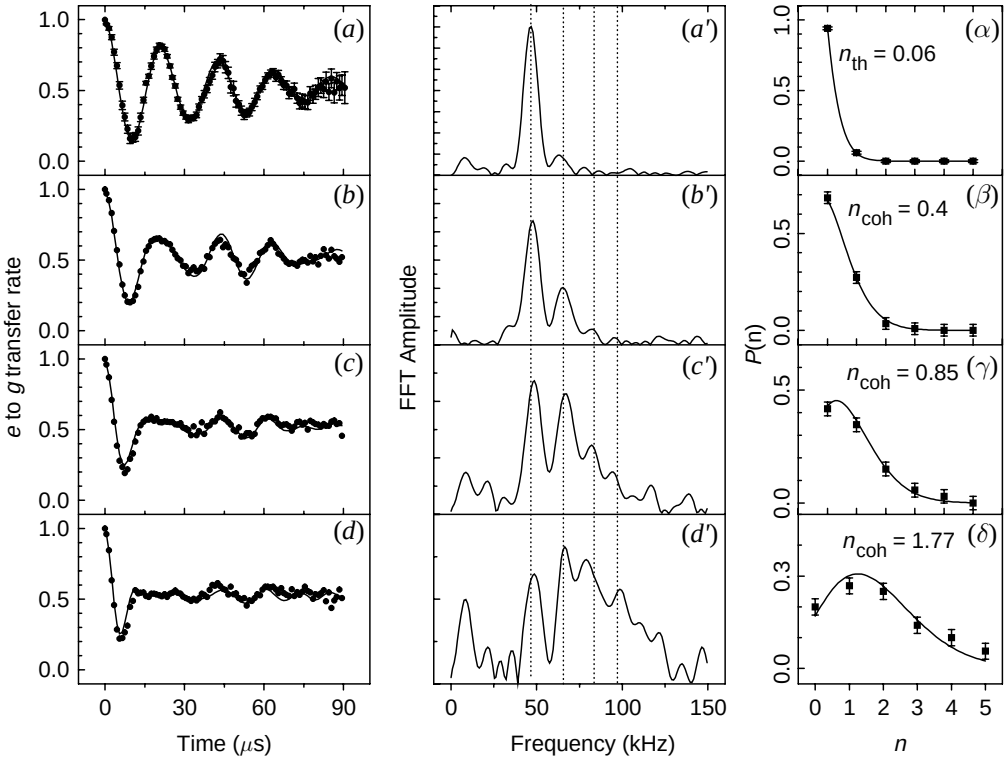

Figure 2. Quantum Rabi oscillations. (a), (b), (c) and (d) Rabi nutation signals. (a) No injected field and 0.06 ($\pm$0.01) thermal photon on average; (b), (c) and (d) coherent fields with 0.40 ($\pm$0.02), 0.85 ($\pm$0.04) and 1.77 ($\pm$0.15) photons on average. The points are experimental; the solid lines are theoretical fits. (a'), (b'), (c'), (d') Corresponding Fourier transforms. Frequencies ranging as the square roots of successive integers are indicated by vertical lines. (α), (β), (γ), (δ) Photon number distribution inferred from experimental signals (points). Solid lines: theoretical thermal (α) or coherent ((β), (γ), (δ)) distributions.

is essentially in vacuum (save for a very small thermal field). Four complete Rabi oscillations are observed, at the expected frequency $\Omega/2\pi$ close to 50 kHz. In fact, the Rabi oscillation experienced by each atom occurs at a frequency $\Omega(\boldsymbol{r})$, which varies with the position of the atom flying across C. The observed Rabi angle corresponds to the accumulated evolution integrated over the atom's flight. It is convenient to define an effective interaction time t by equating the accumulated Rabi phase to Ωt, where Ω is the Rabi coupling at cavity centre. This is the time t represented on the x-axis in figure 2. The observed oscillation corresponds to the coupling of the $|e,0\rangle$ and $|g,1\rangle$ states of the 'atom + field' system and describes the reversible evolution of the atom between e and g, correlated to the emission and absorption of one photon in C. It can be interpreted in the coupled oscillator model of the Thomson theory of atom–matter interaction, as resulting from the resonant coupling of the atom and field 'oscillators' which reversibly exchange their energy. The damping of the oscillation is due to the inhomogeneity of the Rabi frequency across the atomic beam diameter, to detectors imperfections as well as to various decoherence processes including cavity and atom damping. Note that this vacuum Rabi oscillation signal is the time domain counterpart of the vacuum Rabi splitting observed in the spectrum of the atom–empty cavity system (Thompson *et al.* 1992; Bernardot *et al.* 1992).

Figures 2*b–d* show the Rabi oscillation signal when the cavity contains a coherent field with an average photon number equal, from top to bottom, to $n = 0.40$ (± 0.02), 0.85 (± 0.04) and 1.77 (± 0.15). The signal becomes then a superposition of several frequency components, which correspond to the various photon numbers present in the field. The points are experimental and the lines are theoretical fits. The beating between these components gives rise to collapse and revival of the oscillations, which have been predicted by Eberly *et al.* (1980). The Fourier transforms of the Rabi signals, shown in figures 2a'–d', exhibit peaks at the frequencies $\Omega\sqrt{n+1}$ corresponding to the Rabi frequency in the field of n photons ($n = 0$ to 3). These signals thus demonstrate clearly that the Rabi frequency, classically proportional to the field amplitude, is in fact a discrete quantity, providing a direct evidence of field quantization in a box. Note in figure 2a' the small peak at $\Omega\sqrt{2}$ which is an evidence for the presence of a very small residual thermal field in the cavity (average blackbody photon number at 0.6 K: 0.05). Figures 2α–δ show the distribution of the Fourier components amplitudes, which exhibit directly the photon number distributions in the small thermal field (figure 2α) and in the coherent fields with increasing amplitudes (figure 2β–δ, Poisson distribution).

(*b*) *Quantum memory with a single photon in the cavity*

Let us come back to the situation in which an atom interacts with an empty cavity during an effective time t such that $\Omega t = \pi$. The atom exits then with unit probability the cavity in level g, leaving a single photon in it. This photon can be read out after a delay T by sending another atom in level g. If the interaction time of this atom with C is also π/Ω, it absorbs the photon in a time reversed process and ends up in e. This is revealed by measuring the joint probability P_{ge} to detect the first atom in g and the second in e, which must be equal to unity. In fact, there is a finite probability, $\exp(-T/T_{\mathrm{cav}})$, that the photon has decayed between the two atoms, resulting in the second atom remaining in level g. Thus, P_{ge} evolves from one to zero when the delay between the two atoms is increased. We have observed this effect and measured in this way directly the decay of a single photon in C (Maître *et al.* 1997).

We have also sent in the empty cavity C an atom subjected in R_1 to a $\frac{1}{2}\pi$ pulse of microwaves (frequency ν). The atom is thus prepared before entering C in a superposition of e and g states with equal weights. If the condition $\Omega t = \pi$ is satisfied, the e part of the atom's wave function emits with unit probability a photon in C, while the g part remains unaltered. As a result, the atomic state superposition is mapped onto the field, as a superposition of 0 and 1 photon states, while the atom ends up in level g. We prepare in this way a field in C which has an average photon number equal to $\frac{1}{2}$, and a well-defined phase, directly related to the phase of the classical microwave field in R_1. The atom has been used as a carrier of phase information from R_1 to C.

In order to read out this information, we send after a delay T a second atom, prepared in level g, which again undergoes a π pulse in C. The quantum coherence is then mapped onto this atom, as a superposition of e and g states, and the cavity ends up empty. In order to reveal this coherence, we apply a $\frac{1}{2}\pi$ pulse of classical microwave to the second atom in R_2, this pulse having the same frequency ν and phase as the one applied on the first atom in R_1. The cavity R_2 followed by the energy counters acts as a detector of the second atom's coherence. The probability of detecting this atom in e or g exhibits oscillations versus ν. These oscillations are

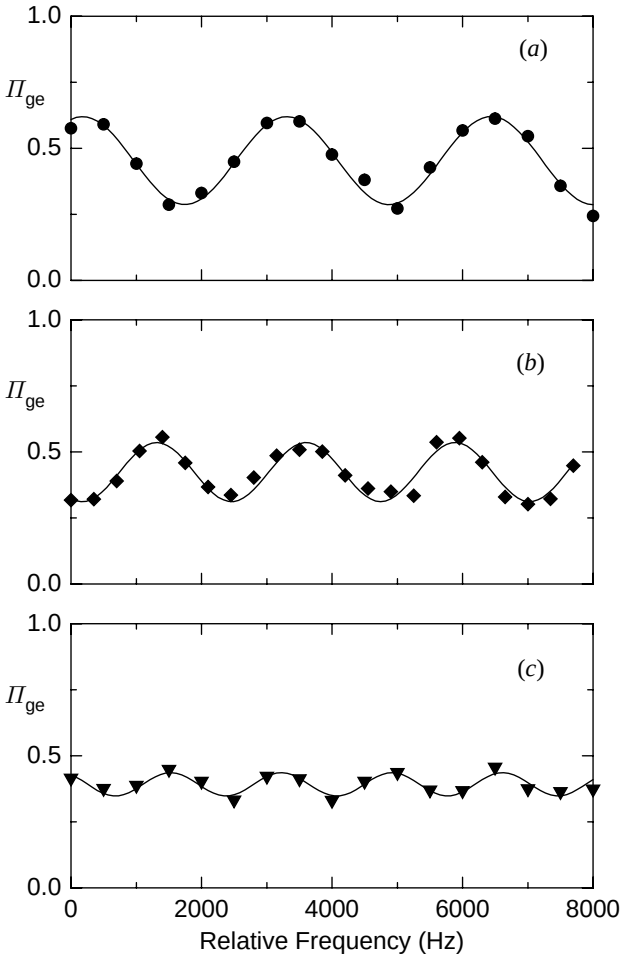

Figure 3. Transfer of coherence between two atoms: conditional probability $\Pi_{ge}(\nu)$ of detecting the second atom in e provided the first one is detected in g versus the frequency ν of the microwave pulses applied to the first atom in R_1 and to the second in R_2. The delay between the two microwave pulses in R_1 and R_2 are 301, 436 and 581 μs, respectively, from (a) to (c).

reminiscent of the usual Ramsey fringes observed when a single atom is subjected to two pulses of microwaves at different times (Ramsey 1985). Here, however, the two pulses are acting on two different atoms and the coherence is transferred between them via the cavity field in C. Figures 3*a–c* show the fringe signals which reveal this coherence transfer, for three different time intervals between the atoms. Note that when this time is increased, not only the fringe period, but also the fringe amplitude decreases. This decrease reveals the field decay in the cavity. We measure by this experiment the field amplitude, and not, as before, the field energy damping, which explains that we find a characteristic decay time of the fringe amplitude twice as long as that in the previously described single photon experiment (Maître *et al.* 1997).

In these resonant atomic correlation experiments, a quantum information, which can be described as a qubit (DiVincenzo 1995; Ekert 1996), is transferred between two atoms via a one photon field stored in the cavity. In the end, the cavity field is restored to its vacuum state and the cavity acts as a catalyst in the process, which can be described as the operation of a quantum memory. Such a mapping process

will be essential in the implementation of a cavity QED quantum gate (experiment in progress, Domokos *et al.* 1995).

(*c*) *Cavity induced atom–atom entanglement*

The cavity can also be used to prepare non-local entanglement between an atom and the field or between two atoms, according to a method proposed by Cirac & Zoller (1994). Let us send a first atom in level e across an empty cavity, the effective atom–cavity interaction time being such that $\Omega t = \frac{1}{2}\pi$. The atom has then equal probabilities to stay excited or to decay to level g while emitting a single photon in C. The system ends up after the interaction in the entangled state $|e,0\rangle - |g,1\rangle$. This entanglement can be transformed into an atom–atom correlation by sending a second atom prepared in g across C, setting the interaction time so that $\Omega t = \pi$. The photon left by the first atom is then absorbed by the second one with unit probability, leaving the cavity empty and the atoms in the entangled state

$$|\Psi_{\mathrm{EPR}}\rangle = \tfrac{1}{\sqrt{2}}(|e_1, g_2\rangle - |g_1, e_2\rangle), \tag{3.1}$$

where the indices label the first and the second atom, respectively. The cavity is a catalyst entangling the two atoms.

The entangled atom system is an exact analogue of the spin pair described in the original Einstein–Podolsky–Rosen article (Einstein *et al.* 1935). One can assimilate each of the two atoms with a spin-$\frac{1}{2}$ particle, the e and g states corresponding to the $+\frac{1}{2}$ and $-\frac{1}{2}$ states quantized along a direction $0z$. The entangled pair is the rotationally invariant 'spin zero' state of the system. It can equivalently be expressed in any basis corresponding to another quantization direction. If the new axis is taken in the $x0y$ plane instead of $0z$, in a direction making an angle ϕ with $0x$, the new spin eigenvectors are of the form $|e\rangle + \mathrm{e}^{\mathrm{i}\phi}|g\rangle$ and the same entangled pair can be written (within an irrelevant overall phase factor) as

$$|\Psi_{\mathrm{EPR}}\rangle = \tfrac{1}{\sqrt{2}}[(|e_1\rangle + \mathrm{e}^{\mathrm{i}\phi}|g_1\rangle)(|e_2\rangle - \mathrm{e}^{\mathrm{i}\phi}|g_2\rangle) - (|e_1\rangle - \mathrm{e}^{\mathrm{i}\phi}|g_1\rangle)(|e_2\rangle + \mathrm{e}^{\mathrm{i}\phi}|g_2\rangle)]. \tag{3.2}$$

Equations (3.1) and (3.2) express a perfect anticorrelation between the states of the two atoms, whichever basis is chosen for the detectors. It cannot be explained by classical arguments, which is the essence of the EPR paradox.

We have performed two-atom counting experiments to demonstrate these correlations (Hagley *et al.* 1997). To analyse the entanglement in the energy basis, we directly detect the state of the atoms after they leave C, without using R_1 and R_2. Ideally, we should find that the joint probabilities to detect the atoms in the various combinations of e and g levels are $P_{eg} = P_{ge} = \frac{1}{2}$, $P_{ee} = P_{gg} = 0$. We find instead experimentally $P_{eg} = 0.44$, $P_{ge} = 0.27$, $P_{ee} = 0.06$, $P_{gg} = 0.23$. The difference with the ideal case is due to the photon decay between the two atoms as well as imperfections in the Rabi pulses. A quantitative analysis of the experiment shows that we prepare EPR pairs with a 63% purity (Hagley *et al.* 1997).

In order to detect the 'transverse' entanglement described by equation (3.2), we subject both atoms, after they have interacted with C and before detecting their energy, to a $\frac{1}{2}\pi$ pulse in R_2. Note that R_1 is not used in this experiment. The succession of R_2, followed by D_e and D_g, amounts to a detector of the atomic coherent superpositions $|e\rangle + \mathrm{e}^{\mathrm{i}\phi}|g\rangle$, where ϕ is the phase of the pulses applied in R_2.

If both atoms were crossing R_2 simultaneously, one would again expect, according to equation (3.2), a perfect anticorrelation between the e and g detectors. In fact, the detection of the first atom in e immediately 'collapses' the second atom into

the anticorrelated state which corresponds to an instantaneous detection in g. The second atom coherence precesses, however, during the time interval between the two detection events. Depending upon the phase accumulated between the atomic coherence and the microwave pulses in R_2, the probability of detecting the second atom in e or g should vary between 0 and 1. This modulation is again reminiscent of a Ramsey fringe signal. However, the two microwave pulses are applied to different atoms and the modulation reveals the non-local correlations between them.

This oscillation, shown in figure 4, is observed in the conditional probability Π_{e_1,e_2} of detecting the second atom in e, knowing that the first was found in e (dashed line), and also in the conditional probability Π_{g_1,e_2} of finding the second atom in e knowing that the first was detected in g (solid line). The two modulations are in phase opposition. Detecting the first atom in g sets indeed the second atom coherence with an initial phase opposite to the one obtained if the first atom was detected in e. Note that the fringe contrast is only 25%, far from the ideally expected value of 100%. We attribute the reduced contrast to photon decay in C between the two atoms, as well to imperfections in the various Rabi pulses.

This experiment is to our knowledge the first one in which atoms have been entangled at a distance (the maximum separation was 1.5 cm). Other proposals to entangle atoms and to investigate Bell's inequalities with atom pairs have been made (Fry *et al.* 1995). By combining resonant and dispersive interactions, one could generalize this scheme to more than two atoms and prepare, for example, triplets of entangled atoms of the form $|e,e,e\rangle - |g,g,g\rangle$ (Greenberger *et al.* 1990; Cirac & Zoller 1994; Haroche 1995). The manipulation by cavity QED techniques of many atom entanglement opens the way to new studies of quantum non-locality and tests of generalized Bell's inequalities.

4. Dispersive atom–field coupling: Schrödinger's cats and decoherence

We now turn to dispersive experiments in which the atomic transition frequency ω_0 and the field mode frequency ω differ by a small quantity δ, large compared to Ω and to the cavity line width (typically, $\delta/2\pi$ is varied between 100 and 700 kHz). A pulsed classical microwave source S is used to inject a small coherent field in C (average photon number between zero and ten) and the non-resonant interaction of this field with the atoms is subsequently studied. Energy conservation prevents the emission or absorption of photons by the atoms and their interaction with C becomes purely dispersive. In fact, the vacuum Rabi frequency being a Gaussian function $\Omega(\boldsymbol{r})$ of the atomic position, the atom–field interaction is turned on and off adiabatically as the atom follows the slowly varying field mode envelope. The adiabatic condition makes photon exchange very unlikely, even at small atom–cavity detunings ($\delta/2\pi = 100$ kHz). The atomic transition undergoes a frequency shift equal to $\Omega^2/2\delta$ per photon, while the cavity mode is shifted by $\pm\Omega^2/4\delta$ when a single atom is placed at cavity centre. This shift takes opposite values for an atom in levels e and g (Haroche 1992).

Typical frequency shifts $\Omega^2/8\pi\delta$ of the order of 6 kHz are achievable when $\delta/2\pi =$ 100 kHz, corresponding to index changes $N-1 = \Omega^2/8\omega\delta$ of the order of 10^{-7}. Such an effect is produced by the presence of a single atom in the volume of the cavity mode (about one atom per cm^3). This corresponds to an index per atom about 15 orders of magnitude larger than those produced by 'ordinary atoms' in usual

Figure 4

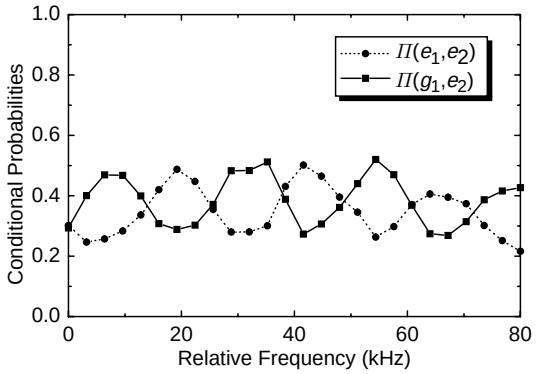

Figure 5

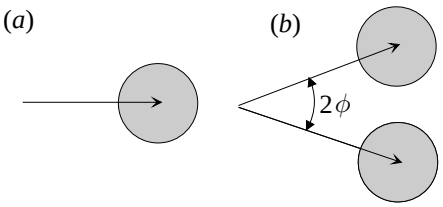

Figure 4. EPR atomic entanglement: conditional probabilities $\Pi(e_1, e_2)$ (circles) and $\Pi(g_1, e_2)$ (squares) of measuring the second atom in level e when the first one has been found in e or g, respectively, plotted versus the frequency ν of the pulses in R_2. The lines connecting the experimental points have been added for visual convenience.

Figure 5. (a) Pictorial representation in phase space of a coherent field state. (b) The two components of the field in equation (4.1) which are correlated to the two atomic states e and g.

transparent media. The field phase shift produced by a single atom is obtained by multiplying the frequency shift at cavity centre by the effective atom–field interaction time. With atoms whose velocities can be varied between 200 and 600 m s^{-1}, this time varies between 15 and 40 μs, corresponding to phase shifts $\Phi = \Omega^2 t/4\delta$ in the range 0.5–1.5 rad. This is quite a macroscopic phase change. The most important feature to consider here is that the single atom index is a quantum object.

This quantum phase shift effect can be used to generate superposition of field states with different phases (Brune *et al.* 1992). A single atom is prepared in a linear superposition of e and g by a $\frac{1}{2}\pi$ pulse in R_1, while a coherent field corresponding to a complex amplitude α is injected in C. When the atom crosses C, it imparts to the field two opposite phase kicks, $\pm\Phi$, depending upon whether it is in e or g. As a result, the combined atom field system becomes

$$|\Psi\rangle = \tfrac{1}{\sqrt{2}}(|e, \alpha e^{i\Phi}\rangle - |g, \alpha e^{-i\Phi}\rangle), \tag{4.1}$$

which describes an entangled atom–cavity state in which the energy of the atom is correlated to the phase of the field. A coherent field can be represented as an arrow in phase space whose length and direction are associated with the amplitude and phase of the field (see figure 5a). The tip of the arrow lies in a circle of unit radius describing the conjugated uncertainties in field amplitude and phase. Equation (4.1) indicates that this arrow is in fact a 'meter' which assumes two different directions when the atom is in e or g (figure 5b). One can say that the dispersive interaction realizes an essential step in a 'measurement' process in which the 'field arrow' is used to determine the atom's energy. One can also adopt Schrödinger's metaphor (Schrödinger 1935) and say that the $+\Phi$ and $-\Phi$ field components are laboratory versions of the 'live' and 'dead' states of the famous cat trapped in a box with an atom in a linear superposition of its excited and ground states.

After C, the atom undergoes another $\frac{1}{2}\pi$ pulse in R_2, phase coherent with the pulse in R_1 and is detected by D_e or D_g. Repeating the experiment many times, we reconstruct the probability of detecting the atom in g versus the frequency ν applied in R_1 and R_2. The experiment (Brune *et al.* 1996*b*) is performed either with

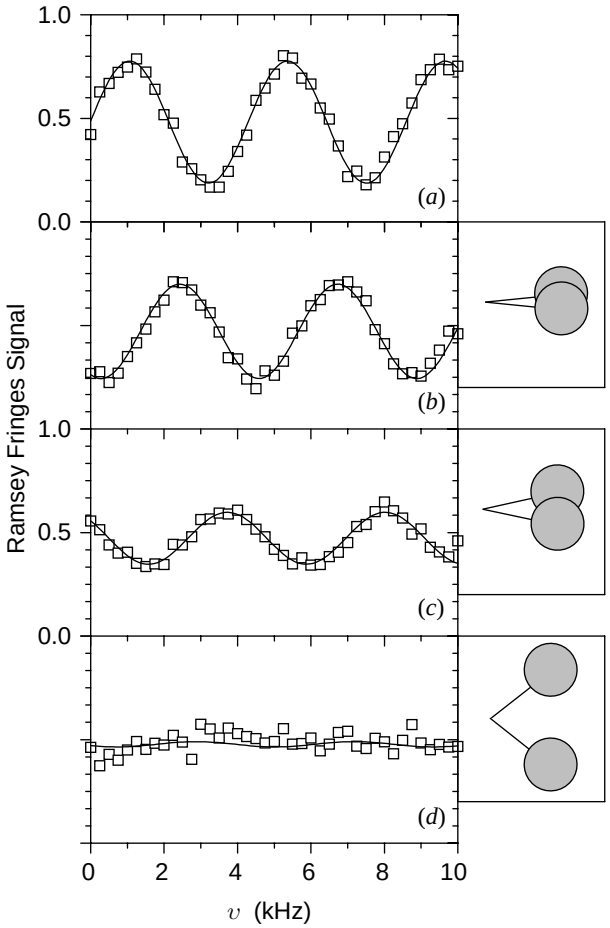

Figure 6. Ramsey fringes in the probability versus ν of detecting the atom in level g: (a) C empty, $\delta/2\pi = 712$ kHz; (b)–(d) C stores a coherent field with $|\alpha| = \sqrt{9.5} = 3.1$, $\delta/2\pi = 712$, 347 and 104 kHz, respectively. Points are experimental and curves are sinusoidal fits. Inserts show the phase space representation of the field components left in C.

an empty cavity detuned by $\delta/2\pi = 712$ kHz (figure 6a), or with a cavity containing initially a coherent field with an average of 9.5 photons, with decreasing values of the detuning δ (figure 6b–d). The fringes observed when the cavity is empty are a typical Ramsey signal, which can be interpreted as an atomic interference effect. The atom can be transferred from e to g either in R_1 (in which case it crosses C in level g) or in R_2 (it then crosses C in level e). Since the two 'paths' cannot be distinguished, the corresponding amplitudes interfere, leading to fringes in the final probability (figure 6a).

When a coherent field is initially present in C, it gets a phase kick which could allow us to determine in principle the state of the atom when it was in C. Such a measurement, even if it remains virtual, must, according to the complementarity principle (Scully *et al.* 1991; Haroche 1992; Pfau *et al.* 1994; Chapman *et al.* 1995), destroy the interference effect and wash out the Ramsey fringes. If δ is relatively large, and Φ accordingly small (figure 6b), the field components overlap so that the 'measurement' of the atom's energy remains ambiguous. The potential knowledge of

the atomic path is only partial and the fringes remain visible, albeit with a reduced contrast. This contrast decreases further when δ becomes smaller (figure 6*c*) and vanishes altogether when δ is so small that the overlap between the field components is negligible (figure 6*d*). The vanishing of the fringe contrast demonstrates that a field with non-overlapping components has been prepared in C. A quantitative analysis shows that the fringe signal is fully described by the overlap integral between the two field components, its modulus yielding the fringe contrast and its phase fixing the phase of the Ramsey fringes. From this phase shift (clearly observable in figure 6 when Φ is changed) we can deduce the average number of photons in C ($n = 9.5$ in this experiment).

Theory predicts that coherent field states superpositions of the kind described by equation (4.1) are fragile and subject to decoherence, when the number of photons, or the angle Φ between the field components, become large (Zurek 1981, 1982; Caldeira & Leggett 1983; Joos & Zeh 1985; Walls & Milburn 1985; Brune *et al.* 1992; Omnès 1994; Goetsch *et al.* 1996). In order to check the coherence of the superposition and to study how it gets transformed with time into a mere statistical mixture, we have probed the 'cat state' with a second atom, crossing the cavity after a delay following a proposal of Davidovich *et al.* (1996). The probe has the same velocity as the first atom and produces identical phase shifts. Since it is also prepared into a superposition of e and g, it again splits into two parts each of the field components produced by the first atom.

The final field state exhibits then four components, two of which coincide in phase. Whether the two atoms have crossed C in the e, g, or in the g, e combination, the net result is to bring back the phase of the field to its initial value. After the atomic states have been mixed again in R_2, there is no way to tell in which state the atoms have crossed C (e, g or g, e combination), since the second atom has partially erased the information left by the first one in the field (Scully & Walther 1989). As a result, two 'paths' associated with the atom pair are indistinguishable. The contributions corresponding to the e, g and g, e paths lead, in the joint probabilities P_{ee}, P_{eg}, P_{ge} and P_{gg}, to the presence of interfering terms. It is convenient to define an atomic correlation signal η by the following combination of joint probabilities:

$$\eta = \frac{P_{ee}}{P_{ee} + P_{eg}} - \frac{P_{ge}}{P_{ge} + P_{gg}}. \tag{4.2}$$

If the state superposition survives during the time interval T between the atoms, η ideally takes the value $\frac{1}{2}$, whereas it vanishes when the state superposition is turned into a statistical mixture. The result of the η measurement versus T is shown in figure 7 for two different 'cat' states produced by the first atom (these states are depicted in the inserts). The points are experimental and the curves theoretical. The maximum correlation signal is 0.18, and not 0.5, because of the limited fringe contrast of our Ramsey interferometer. We see that decoherence occurs within a time much shorter than the cavity damping time and is more efficient when the separation between the cat components is increased. The agreement between experiment and theory is quite good.

This decoherence process is due to the loss of photons escaping from the cavity via scattering on mirror imperfections. Each escaping photon can be described as a small 'Schrödinger kitten' copying in the environment the phase information contained in C (Zurek 1997). The mere fact that this 'leaking' information could be read out to determine the phase of the field is enough to wash out the interference effects related

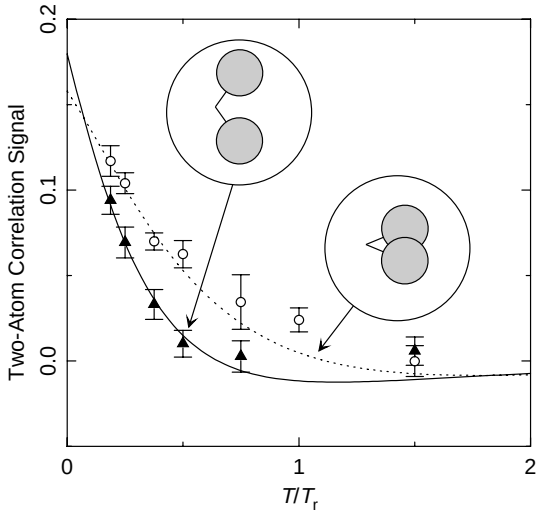

Figure 7. Decoherence of a Schrödinger cat: two-atom correlation signal η versus T/T_r for $\delta/2\pi = 170$ kHz (circles) and $\delta/2\pi = 70$ kHz (triangles). Dashed and solid lines are theoretical. Inserts: pictorial representations of corresponding field components separated by 2Φ.

to the quantum coherence of the 'cat' state. In this respect, we understand that decoherence is also a complementarity phenomenon. The short decoherence time of our Schrödinger cat, of the order of $T_{\rm cav}/n$, is also explained by this approach. The larger the photon number, the shorter is the time required to leak a single 'photon-copy' in the environment. This experiment verifies the basic features of decoherence and vividly exhibits the fragility of quantum coherences in large systems.

5. Conclusion

These experiments are first steps towards more elaborate manipulations of systems made of a few atoms and photons in situations where the coupling to the environment can be minimized and, to some extent, controlled. We are planning to entangle more atoms, to study Schrödinger cat states with larger photon numbers and to prepare field states delocalized in two or more separate cavities. The time evolution of these systems will be studied and ways to slow down their decoherence or to reverse its effects will be investigated. Other groups are exploring related Cavity QED phenomena in the microwave (Raithel *et al.* 1994) or in the optical domains (Kimble 1994). Strong similarities also exist between our experiments and the one being performed or planned with ions oscillating in a trap (Monroe *et al.* 1995; Cirac *et al.* 1996). In the latter case, the internal states of the ions are entangled to the vibrational degrees of freedom of the ions, which replace the field excitation of the Cavity QED experiments. The hamiltonians describing the evolution of these systems look very much alike. From both kinds of experiments, we are bound to learn more about the transition from quantum to classical behaviour in mesoscopic systems (Zurek 1981, 1982, 1991, 1997).

References

Berman, P. 1994 *Cavity quantum electrodynamics*. New York: Academic.

Bernardot, F., Nussenzveig, P., Brune, M., Raimond, J. M. & Haroche, S. 1992 *Europhys. Lett.* **17**, 33.

Brune, M., Haroche, S., Davidovich, L. & Zagury, N. 1992 *Phys. Rev.* **A45**, 5193.

Brune, M., Schmidt-Kaler, F., Maali, A., Dreyer, J., Hagley, E., Raimond, J. M. & Haroche, S. 1996*a* *Phys. Rev. Lett.* **76**, 1800.

Brune, M., Hagley, E., Dreyer, J., Maître, X., Maali, A., Wunderlich, C., Raimond, J. M. & Haroche, S. 1996*b* *Phys. Rev. Lett.* **77**, 4887.

Caldeira, A. O. & Leggett, A. J. 1983 *Physica* A **121**, 587.

Chapman, M. S., Hammond, T. D., Lenef, A., Schmiedmeyer, J., Rubenstein, R. A., Smith, E. & Pritchard, D. E. 1995 *Phys. Rev. Lett.* **75**, 3783.

Cirac, J. I. & Zoller, P. 1994 *Phys. Rev.* A **50**, R2799.

Cirac, J. I., Parkins, S., Blatt, R. & Zoller, P. 1996 In *Advances in atomic and molecular physics*, vol. 37, p. 238. New York: Academic.

Davidovich, L., Brune, M., Raimond, J. M. & Haroche, S. 1996 *Phys. Rev.* A **53**, 1295.

DiVicenzo, D. P. 1995 *Science* **270**, 255.

Domokos, P., Raimond, J. M., Brune, M. & Haroche, S. 1995 *Phys. Rev.* A **52**, 3554.

Eberly, J. H., Narozhny, N. B. & Sanchez-Mondragon, J. J. 1980 *Phys. Rev. Lett.* **44**, 1323.

Einstein, A., Podolsky, B. & Rosen, N. 1935 *Phys. Rev.* **47**, 777.

Ekert, A. & Josza, R. 1996 *Rev. Mod. Phys.* **68**, 3733.

Fry, E. S., Walther, T. & Li, S. 1995 *Phys. Rev.* A **52**, 4381.

Greenberger, D. M., Horne, M. A. & Zeilinger, A. 1990 *Am. J. Phys.* **58**, 1131.

Goetsch, P., Graham, G. & Haake, F. 1996 *Quantum Semiclass. Opt.* **8**, 157.

Hagley, E., Maître, X., Nogues, G., Wunderlich, C., Brune, M., Raimond, J. M. & Haroche, S. 1997 *Phys. Rev. Lett.* **79**, 1.

Haroche, S. 1992 Cavity quantum electrodynamics. In *Fundamental systems in quantum optics, Les Houches summer school session LIII* (ed. J. Dalibard, J. M. Raimond & J. Zinn-Justin). Amsterdan: North Holland.

Haroche, S. 1995 In *Fundamental problems in quantum theory* (ed. D. Greenberger & A. Zeilinger). *Ann. N.Y. Acad. Sci.* **755**, 73.

Haroche, S., Brune, M. & Raimond, J. M. 1992 *Appl. Phys.* B **54**, 355.

Haroche, S., Goy, P., Raimond, J. M., Fabre, C. & Gross, M. 1982 *Phil. Trans. R. Soc. Lond.* A **307**, 659.

Hulet, R. G. & Kleppner, D. 1983 *Phys. Rev. Lett.* **51**, 1430.

Joos, E. & Zeh, H. D. 1985 *Z. Phys.* B **59**, 223.

Kimble, H. J. 1994 In *Cavity quantum electrodynamics* (ed. P. Berman), p. 203. New York: Academic.

Maître, X., Hagley, E., Nogues, G., Wunderlich, C., Goy, P., Brune, M., Raimond, J. M. & Haroche, S. 1997 *Phys. Rev. Lett.* **79**, 769.

Monroe, C., Meekhof, D. M., King, B. E., Itano, W. M. & Wineland, D. J. 1995 *Phys. Rev. Lett.* **75**, 4714.

Nussenzveig, P., Bernardot, F., Brune, M., Hare, J., Raimond, J. M., Haroche, S. & Gawlik, W. 1993 *Phys. Rev.* A **48**, 3991.

Omnès, R. 1994 *The interpretation of quantum mechanics*. Princeton University Press.

Pfau, T., Spälter, S., Kurtsiefer, Ch., Ekstrom, C. R. & Mlynek, J. 1994 *Phys. Rev. Lett.* **73**, 1223.

Raithel, G., Wagner, C., Walther, H., Narducci, L. M. & Scully, M. O. 1994 In *Cavity quantum electrodynamics* (ed. P. Berman), p. 57. New York: Academic.

Ramsey N. F. 1985 *Molecular beams*. Oxford University Press.

Schrödinger, E. 1935 *Naturwissenschaften* **23**, 807, 823, 844.

Scully, M. O. & Walther, H. 1989 *Phys. Rev.* A **39**, 5299.

Scully, M. O., Englert, B.-G. & Walther, H. 1991 *Nature* **351**, 111.

Thompson, R. J., Rempe, G. & Kimble, H. J. 1992 *Phys. Rev. Lett.* **68**, 1132.
Walls D. F. & Milburn, G. J. 1985 *Phys. Rev.* A **31**, 2403.
Zurek, W. H. 1981 *Phys. Rev.* D **24**, 1516.
Zurek, W. H. 1982 *Phys. Rev.* D **26**, 1862.
Zurek, W. H. 1991 *Phys. Today* **44**, 36.
Zurek, W. H. 1997 *Phys. World* **January**, 25.